RSC Advances

PAPER

View Article Online
View Journal | View Issue

Cite this: *RSC Adv.*, 2020, **10**, 12035

Enhancement performance of application mussel-biomimetic adhesive primer for dentin adhesives†

Jiahui Zhang,[a] Ying Zhao,[a] Zilu Tian,[a] Jiufu Zhu,[b] Zuosen Shi,[b] Zhanchen Cui*[b] and Song Zhu*[a]

Received 29th December 2019
Accepted 17th March 2020

DOI: 10.1039/c9ra10992g

rsc.li/rsc-advances

In this study, we evaluated bioinspired adhesive primers for durable adhesion between dentin and composite resins. *N*-3,4-Dihydroxyphenethyl methacrylamide (DMA) primer monomer (small bifunctional group molecules containing catechol and acrylic groups at opposite ends) was prepared to mimic the interaction between the catechol group and the mineral interface of marine mussels. The shear bonding strength, microleakage, degree of conversion, contact angle, and compatibility were tested. The shear bond strength was significantly improved, and microleakage was diminished after the application of the DMA primer. However, the degree of conversion was decreased. The wettability of the dentin was enhanced, and the DMA primer showed no negative influence on cell proliferation. The results of this study showed the possibility of using DMA primers in clinical practice. This may provide a new strategy for improving adhesion durability.

Introduction

Composite resins are widely used in dental restorations due to their aesthetic properties and direct filling properties.[1–5] Strong and durable bonding to the tooth is the key factor in successfully repairing defects.[6–9] However, the oral environment is challenging, and multiple factors interact to limit the life of the restoration. It has been found that the weak link of composite resin restoration lies in the dentin–adhesive interface,[9] and secondary caries are the main reason for the failure of restoration.[9–14]

The mechanism of dentin bonding is the penetration of adhesive monomer into the demineralized dentin collagen matrix, forming a hybrid layer (HL).[6–9] The adhesive forms not only a bond between the tooth and the composite resin but also a barrier to protect the demineralized collagen fibers from hydrolysis and attack from bacteria and enzymes in the oral cavity.[9,15,16] Therefore, strong bonding and good sealing properties, which can reduce microleakage, play an important role in the long-term stability and durability of a dentin adhesive.

The hostile environment in which marine mussels live is similar to the oral cavity, which is characterized by continuous turbulence, tidal washing and temperature changes. However, the wave-swept rocky shores are home to a large number of marine mussels, and these sessile organisms can attach themselves to underwater surfaces, forming mussel beds as ecosystems and individual-level self-assembly systems.[17–20] Mussels secrete protein-based holdfast (byssus), whose distal byssal plaque is specifically used for bonding, allowing them to bond strongly to underwater surfaces, as shown in Fig. 1(A). It is known that more than 10 types of adhesive holdfast proteins have been found in the Mytilus genus, including mussel foot protein (mfp) 1–6 and collagen,[21–23] among which mfp-3 and mfp-5 act as surface primers between mussel byssal plaque and rock surfaces,[21,24,25] as shown in Fig. 1(B). These interfacial mfps have an unusually high content (28–34%) of benzene ring residues, including tyrosine, tryptophan, and post translationally modified products of tyrosine: 3,4-dihydroxyphenyl-L-alanine (DOPA), as shown in Fig. 1(C) and (D). DOPA is considered to be the most important functional group of wet bonding because of its strong bidentate binding on oxidized mineral surfaces.[21] To obtain strong bonding properties, natural mfps were extracted from marine mussels by tissue engineering, which was very inefficient and expensive.[26,27] This prompted us to study a synthetic mussel biomimetic polymer providing water-resistant and strong bonding properties.

Drawing inspiration from natural marine mussels, many research laboratories have attempted to convert this natural bioadhesive into a synthetic adhesive containing catechol functional groups for different fields, such as multifunctional polymer coatings,[28] medical sealants,[29] self-healing polymers in aqueous media[30] and ultralow fouling coatings.[31] In the field of dental materials, only a few studies have been carried out. Sang-Bae Lee *et al.* synthesized a biomimetic dental adhesive polymer for wet bonding to reduce complications caused by saliva contamination during bonding.[32] B. Kollbe Ahn and colleagues prepared a catecholic primer for the surface of inorganic fillers,

[a]*Department of Prosthetic Dentistry, School and Hospital of Stomatology, Jilin University, Changchun 130021, P. R. China. E-mail: zhusong1965@163.com*

[b]*State Key Lab of Supramolecular Structure and Materials, College of Chemistry, Jilin University, Changchun 130021, P. R. China*

† Electronic supplementary information (ESI) available. See DOI: 10.1039/c9ra10992g

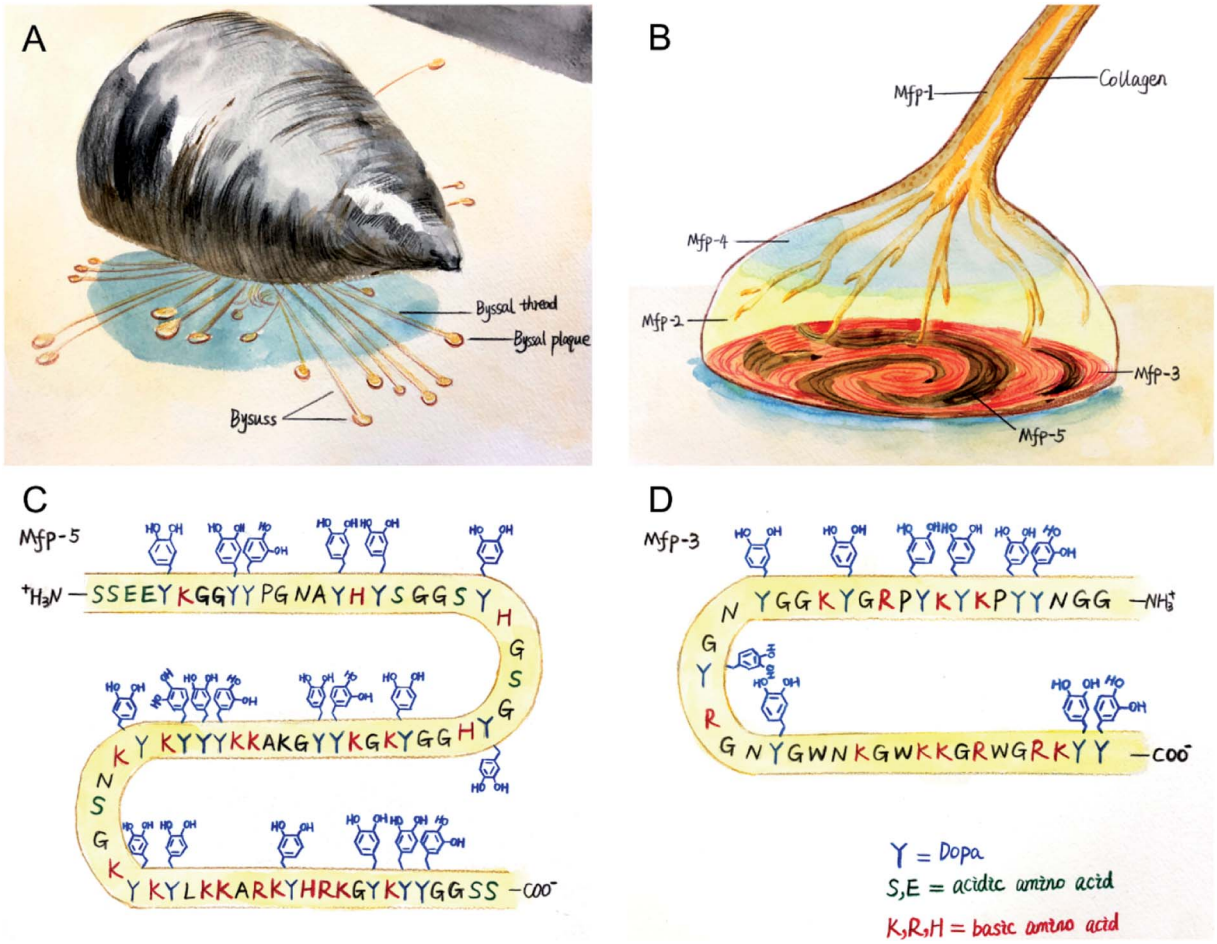

Fig. 1 (A) A mussel anchored by byssal threads and plaques to a substrate. (B) Schematic of the distribution of major mfp's in byssal plaque. (C) Primary sequence of mfp-5. (D) Primary sequence of mfp-3.

improving the connection between the filler and the organic resin and enhancing the mechanical properties compared with silane coupling agents.[33] Although previous studies have shown that bioadhesives modified with catechol groups exhibited significant improvement in bonding properties, their bonding strength is far less than natural mussels, which originated from poor consideration of the multiplex structure of mussels.[34] For example, although the content of catechol groups in the interfacial mfp (mfp-3, 5) is as high as 20–28%, the content in the bulk mfps is greatly reduced, at only 2–5 mol%. However, the main research of mussel-mimic wet adhesion has focused on introducing a catechol functional group that can promote adhesion between the surface of the substrate and mussel byssal plaque into the adhesive polymer.[35–37] In contrast, mussel biomimetic bonding research rarely attempts to simulate the natural bonding process of mussels, creating interfacial primers to improve the bonding performance, similar to nature.[38–40] According to a study of Dr B. Kollbe Ahn's research group, with the application of a single molecule priming layer of a catechol group, the bonding strength of cross-linking polymethacrylic resin to a mineral filler surface can be significantly improved compared with conventional silane coupling agents and phosphate coupling agents.[40]

Inspired by marine mussels, this study prepares a small molecule of dopa analogs (a small bifunctional group molecule, including a catechol group and an acrylic group at the opposite ends) serving as an adhesive primer for the chemical cross-linking of two different materials using a mussel priming bonding strategy mechanism. Shear strength testing and microleakage experiments are performed to verify whether an application of the catecholic primer can increase the strength of dental adhesive and reduce the occurrence of microleakage. At the same time, biocompatibility experiments were also tested.

Materials and methods

1 Materials

Spectrum bond (Dentsply DeTrey GmbH, De-Trey-Strasse1, 78467 Konstanz, Germany), Single bond universal (3M ESPE, St. Paul, MN, USA), Adper single bond 2 (3M ESPE, St. Paul, MN, USA), and Filtek Z350XT (3M ESPE, St. Paul, MN, USA) were used. L929 cells were obtained from the School of Life Science, Jilin University. 3-(4,5-Dimethylthiazole-2-yl)-2,5-diphenyltetrazolium bromide (MTT) was purchased from Sigma Aldrich. Methylene blue was purchased from Aladdin. All other chemical reagents were analytical grade and provided by Aladdin.

2 Preparation and characterization of *N*-3,4-dihydroxyphenethyl methacrylamide (DMA) monomer

The synthesis method was carried out according to a previous study.[41] Sodium tetraborate ($Na_2B_4O_7 \cdot H_2O$, 15.8 mmol) and sodium carbonate (Na_2CO_3, 47.2 mmol) were dissolved in deionized water with N_2 bubbling for at least one hour. Then, 3-hydroxytyramine hydrochloride (15.8 mmol) was added into the reaction with continuous N_2 bubbling conditions, after which methacryloyl chloride (63.2 mmol) was added dropwise. Next, 8.6 g Na_2CO_3 was added to adjust the reaction pH to 9. After stirring at room temperature for 12 h, the reaction was completed. It was washed with HCl and a saturated NaCl solution to adjust the pH to 1. The original product was extracted with ethyl acetate (30 mL × 3) followed by drying over anhydrous $MgSO_4$. After suction filtration, the ethyl acetate was removed by a rotary evaporator, and the product was recrystallized by 500 mL *n*-hexane at −20 °C, with a lower layer appearing as a white flocculent product. After the upper layer of the *n*-hexane was poured off, the remaining *n*-hexane was vacuumed in a vacuum oven to obtain white powder (yield = 65%). The synthesis process is shown in Fig. 2.

The structure of the synthesized DMA monomer was characterized by Fourier transform infrared spectroscopy (FTIR) and nuclear magnetic resonance spectrometry (^{1}H NMR spectrum). FTIR was measured by a BRUKER VERTEX 80V infrared spectrometer in a range of 4000–400 cm^{-1}. The ^{1}H NMR spectrum was performed by a Bruker AVANCE 500 MHz type III nuclear magnetic resonance spectrometer using dimethyl sulfoxide (DMSO) as a solvent.

3 Thermal stability characterization

Thermal stability was performed to study the degradation characteristics of the DMA monomer. Thermogravimetric analysis of the DMA monomer sample was determined using a TA Instruments TGA Q500 thermal analyzer with a heating rate of 10 °C min^{-1} in a nitrogen environment from room temperature to 800 °C.

4 Shear bond strength and interfacial failure mode

Specimen preparation. Healthy mandibular bovine incisors with an average age of 3 years were selected without any cracks and caries to ensure the homogeneity of the experiment. The bovine teeth were stored in a 0.5% chloramine T solution and placed in a refrigerator at 4 °C. All teeth were used within 2 weeks. The study was approved by the Ethics Committee for Human and Animal Studies of the Institute of Stomatology of Jilin University. All bovine teeth were randomly grouped. A low-speed saw with a diamond-impregnated disk (IsoMet 1000, Buehler; Lake) exposed the labial surface of the bovine dentin, ensuring the enamel was completely removed. The dentin surface was polished with 1000-grit silicon carbide (SiC) sandpaper under running water cooling. The dentin was etched with 35% phosphoric acid etchant for 15 s, rinsed for 15 s, and continuously air-blown. The experimental group was applied with a layer of DMA primer for 60 s, blown with oil-free condensed air for 5 s before using the adhesive. The control group was directly applied with commercial adhesive according to the manufacturer's instructions. Information on the three common commercial adhesives is shown in Table 1. The specific grouping of the experiment is shown in Table 2 ($n = 10$). Then, Z350XT resin was filled layer by layer in a cylindrical plastic mold (inner diameter = 3.0 mm, thickness = 5 mm), which was placed on the surface of the dentin to make a resin column and light-cured for 40 s using a light-curing unit with a light intensity of 900 mW cm^{-2}. The curing light was monitored by a radiometer before use to ensure light intensity. The mold was removed, and the sample was stored in deionized water at 37 °C for 24 h. The process is shown in Fig. 3. The sample was embedded in a ring-shaped metal aluminum mold ring (diameter = 25 mm) with self-curing plastic. When fully cured, the sample was tested on a universal testing machine to measure the shear strength. All samples were prepared at 23 ± 2 °C and 50 ± 10% relative humidity.

Shear bond strength (SBS) test. A universal testing machine continuously loaded on the sample until it broke with a crosshead speed at 1.0 mm min^{-1}. The bevelled blade with a flat contact surface was contacting the dentin bonding surface as closely as possible. The shear bonding strength was calculated by the maximum load at break divided by the bonding area.

Interfacial bonding failure mode. The fracture mode of the bonding interface was observed under a stereomicroscope. Three failure types were defined: (1) adhesive failure; (2) cohesive failure (including dentin cohesive fracture and composite resin cohesive failure); (3) mixed fracture – partially adhesive and partially cohesive failure.

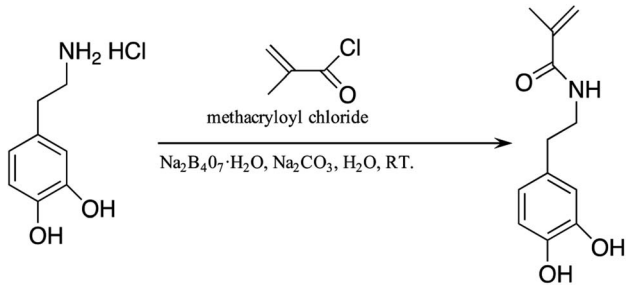

Fig. 2 Illustration of the fabrication process of *N*-3,4-dihydroxyphenethyl methacrylamide (DMA) monomer.

5 Degree of conversion

To investigate the effect of DMA primer on the degree of conversion (DC) of commercial adhesives, the DCs of three adhesives were measured with and without pretreatment with DMA primer (primer solvent: DMSO). The DC was determined by a Fourier transform infrared spectrometer with an attenuated total reflectance accessory ($n = 5$). The FTIR of uncured adhesive was obtained as a control. The adhesive was cured according to the manufacturer's instructions, and the light-polymerized adhesive was immediately subjected to FTIR. DC values were calculated according to the variation of absorbance peak intensity of methacrylate double bonds (C=C, peak at

Table 1 Commercial adhesives for this study[a]

Material	Code	Category	Lot number	Manufacturer	Formulation
Single bond 2	SB2	2-Step etch-and-rinse	N912223	3M ESPE; St. Paul, MN, USA	Bis-GMA, HEMA, dimethacrylates, silica nanofiller, polyalkenoic acid copolymer, initiators, water, ethanol
Spectrum bond	SPB	2-Step etch-and-rinse	1801000919	Dentsply DeTrey GmbH (De-Trey-Strasse1, 78467 Konstanz, Germany)	UDMA, trimethacrylate, PENTA, highly dispersed silicon dioxide, camphorquinone, BHT, cetylamine hydrofluoride, acetone
Single bond universal	SBU	Universal adhesive	4330297	3M ESPE; St. Paul, MN, USA	MDP phosphate monomer, bis-GMA, dimethacrylate resins, HEMA, vitrebond copolymer, fillers, ethanol, water, initiators, silane

[a] Bis-GMA: bisphenol a diglycidyl methacrylate, HEMA: 2-hydroxyethyl methacrylate, UDMA: urethane dimethacrylate, PENTA: phosphoric acid modified acrylate resin, BHT: butylhydroxytoluene, and MDP: methacryloyloxydecyl dihydrogenphosphate.

1636 cm^{-1}) before and after polymerized, and phenyl (peak at 1608 cm^{-1}) was used as the internal standard. The calculation of the DC used the following equation:

$$DC\ \% = \left[1 - \frac{(A_{1636}/A_{1608})\ \text{peak area after curing}}{(A_{1636}/A_{1608})\ \text{peak area before curing}}\right] \times 100\%$$

where A_{1636} and A_{1608} are the absorbance peak area of methacrylate C=C at 1636 cm^{-1} and phenyl at 1608 cm^{-1}, respectively.

6 Contact angle measurements

The bovine incisor was sliced along the crown-root axial using a low-speed saw to obtain a 1 mm thick dentin sheet with no enamel remaining and no perforation. The dentin slice was ground with 1000-grit SiC sandpaper and washed with an ultrasonic machine 2 times for 5 min each to remove debris during cutting and grinding. The dentin was etched with 35% phosphoric acid gel (3M ESPE, St. Paul, MN, USA) for 15 s and rinsed with deionized water for 15 s. The treated samples were randomly divided into two groups ($n = 5$): the dentin surface treated with or without a DMA primer (group of 5% DMA primer). The dentin surface was dried with filtered compressed air at a distance of 1 cm for 60 s. The contact angle was performed using a contact angle meter (Dataphysics OCA20). A 6 μL drop of deionized water was gently placed onto the surface of the dentin. Then, a digital photo was taken, and the contact angle was measured immediately.

7 Microleakage

A standard class V cavity was prepared on the labial surface of a bovine incisor (4 mm wide, 2.0 mm deep, and 3.0 mm high), while a 45 degree edge bevel was prepared. The dentin was etched with 35% phosphoric acid gel for 15 s, rinsed for 15 s, and continuously air-blown with condensed air. The experimental group was applied with a layer of DMA primer for 60 s before using the adhesive. The control group was directly applied with adhesive for 20 s, lightly air-blown for 5 s and cured for 10 s. Three commercial adhesives were divided into 6 groups ($n = 5$). The cavity was filled with Filtek Z350XT composite resin layer by layer and cured for 40 s. After polishing with sandpaper, the sample was stored in deionized water for 24 h. Artificial aging was performed using a thermocycling instrument (PTC2c, Proto-tech, USA) 5000 times by changing the soaking temperature in a 5 °C or 55 °C bath with a dwell time of 30 s. After thermocycling was completed, the root apex was sealed with wax. The entire surface of the tooth was coated with transparent nail polish twice, except for the area within 1 mm of the tooth-restoration interface. A microleakage test was conducted using a standard dye-leakage method. The prepared sample was placed in 1% methylene blue dye for 4 h at 37 °C. The tooth surface was rinsed with deionized water and dried with filter paper. The crown portion was cut into a 1 mm sheet along the tooth long axis under running water cooling using

Table 2 Experimental grouping[a]

Adhesive	Primer	Application time of primer	Figure
SB2	DMSO(control/DMSO/5% DMA/10% DMA/15% DMA)	60 s	Fig. 6(A)
	Ethanol (control/ethanol/5% DMA/10% DMA/15% DMA)		Fig. 6(B)
SPB	DMSO (control/DMSO/5% DMA/10% DMA/15% DMA)	60 s	Fig. 6(C)
	Ethanol (control/ethanol/5% DMA/10% DMA/15% DMA)		Fig. 6(D)
SBU	DMSO (control/DMSO/5% DMA/10% DMA/15% DMA)	60 s	Fig. 6(E)
	Ethanol (control/ethanol/5% DMA/10% DMA/15% DMA)		Fig. 6(F)

[a] Primer formulation: DMSO (control: no primer; DMSO: 1 g DMSO; 5% DMA: 0.05 g DMA + 0.95 g DMSO; 10% DMA: 0.10 g DMA + 0.90 g DMSO; 15% DMA: 0.15 g DMA + 0.85 g DMSO); ethanol (control: no primer; ethanol: 1 g ethanol; 5% DMA: 0.05 g DMA + 0.95 g ethanol; 10% DMA: 0.10 g DMA + 0.90 g ethanol; 15% DMA: 0.15 g DMA + 0.85 g ethanol).

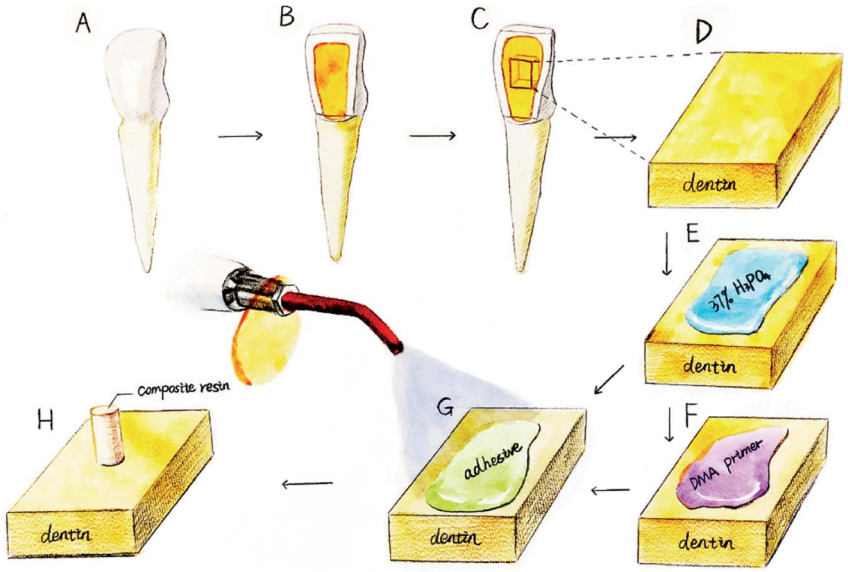

Fig. 3 Specimen preparation of shear bond strength. (A)–(C) The labial surface of bovine dentin was exposed. (D) The dentin block was cut from the tooth. (E) The dentin was etched with 35% phosphoric acid etchant for 15 s. (F) The experimental group was applied with a layer of DMA primer for 60 s, blowed for 5 s before using adhesive. (G) The control group was directly applied with adhesive for 20 s, lightly blown for 5 s, and light-cured for 10 s. (H) Z350XT resin was placed on the surface of dentin to make a resin column and light-cured for 40 s.

a slow-speed diamond saw. The evaluation of microleakage was determined by the depth of dye into the tooth-restoration interface using a stereomicroscope. The depth of leakage of the dye was evaluated by the following criteria:[42]

(0) no obvious dye leakage;

(1) The dye gets to the interface to half the depth of the cavity;

(2) Leakage exceeds half of the depth of the hole but does not involve the axial surface;

(3) Leakage involves the axial surface, but not the pulp;

(4) Leakage involves the pulp.

8 Cytotoxicity test

The DMA primer was radiated by ultraviolet overnight and filtrated to remove bacteria. Then, the DMA primer was diluted serially using Dulbecco's modified Eagle's medium cell culture medium containing 10% fetal calf serum and 1% penicillin and streptomycin at a ratios of 1 : 1000, 1 : 2000, and 1 : 4000 (v/v).[43]

The L929 cells were cultured for an MTT assay. The cells were seeded in a 96-well plate at a density of 1.5×10^4 cells per mL and incubated at 37 °C in 5% CO_2 and 95% relative humidity for 24 h until the monolayer cells were spread over the bottom of the well. The original culture solution was replaced with cell culture medium containing different diluted DMA primers, and the control group was added to the cell culture medium with the surrounding wells sealed with phosphate buffer saline buffer. Then, the cells were continuously incubated for 24 h, 48 h, and 72 h and removed from the incubator. The morphology of the cells was observed under an inverted microscope. Mitochondrial dehydrogenase in living cells enabled the MTT to become insoluble formazan particles that can dissolve in dimethyl sulfoxide (DMSO). Next, 20 μL of MTT solution (5 mg mL^{-1}) was added to each well, and the incubation was terminated after 4 h. Then, 150 μL of DMSO was added to each well, and the 96-well plate was shaken at a low speed for 10 min to fully dissolve the crystal formazan particles. The absorbance was read at a wavelength of 490 nm by a microplate reader (RT-6000, Lei Du Life Science and Technology Co., Shenzhen, China). The control group was regarded as the 100% cell proliferation rate, and the relative growth rate (RGB) of each group was calculated.

The effect of DMA primer on the activity of L929 cells was also evaluated using a live/dead cell staining kit. The cells were seeded at a density of 5×10^4 cells per ml in a 6-well plate for 24 h. After incubation of the diluted DMA primer, the cells were stained with a live/dead cell staining kit according to the manufacturer's instructions. Live cells were stained green, and dead cells were stained red. The 6-well plate was observed under a fluorescence microscope.

9 9 statistical analysis

Data were expressed as the mean ± standard deviation. All statistical data were submitted to one-way analysis of variance (ANOVA) using SPSS software (version 19.0, SPSS Inc., Chicago, IL, USA), given that the data were consistent with a normal distribution. Multiple comparison analysis was conducted using the Tukey test and Dunnett method. The significance level was set at $p = 0.05$ for this study.

Results and discussion

1 Synthesis and characterization of DMA

The ^{1}H NMR spectrum of DMA is shown in Fig. 4(A). The signals in the range of 8.62–8.73 ppm were attributed to the phenolic hydroxyl (Ph–OH) of the catechol group, and the peak at 6.32–6.65 ppm was attributed to the benzene ring (Ph–H). The protons belonging to the amide (N–H) were clearly shown at 7.93 ppm. The resonance peaks at 5.30–5.61 and 1.84 were

assigned to the signal of the vinyl groups ($CH{=}CH_2$), respectively. Additionally, protons from $Ph{-}CH_2{-}$ were apparent with signals at 2.55 ppm. The signal of methylene of $-CH_2-NH-$ appeared at 3.24 ppm. The solvent DMSO peak was observed as a strong signal at 2.50 ppm (integrations and multiplicities of the NMR peaks are provided in ESI†).

DMA was also characterized by FTIR spectra in Fig. 4(B). All relevant FTIR bands are shown in Table S1 (ESI†). The absorption peak at 3367 cm^{-1} can be ascribed to the phenolic hydroxyl (Ph–OH) of the catechol group, indicating that the phenol hydroxyl group was protected by N_2 during the reaction. The N–H stretching vibration at 3201 cm^{-1} wavenumber and the C=O stretching vibration at 1650 cm^{-1} wavenumber were attributed to the amide group, respectively. The spectra of FTIR and ^1H NMR confirmed that DMA containing catechol groups and vinyl groups was successfully synthesized by the reaction between dopamine hydrochloride and methacryloyl chloride, which formed amide covalent bonds.

Direct characterization of the presence of DMA primer on the dentin surface is difficult. It was tested with attenuated total reflection infrared ATR-FTIR, but the results were not obvious. Inspired by a previous research,[33] we demonstrated it in a indirect way. After applying the DMA primer for 60 s, the dentin surface was rinsed with deionized water and washed ultrasonically for 10 min. Then, a NaOH alkaline solution was applied to the dentin surface. The dentin surface color gradually turned brown, indicating that there is still DMA on the dentin surface after rinsing with deionized water and washing with ultrasonic vibration. And the specific connection between DMA and dentin needs further exploration.

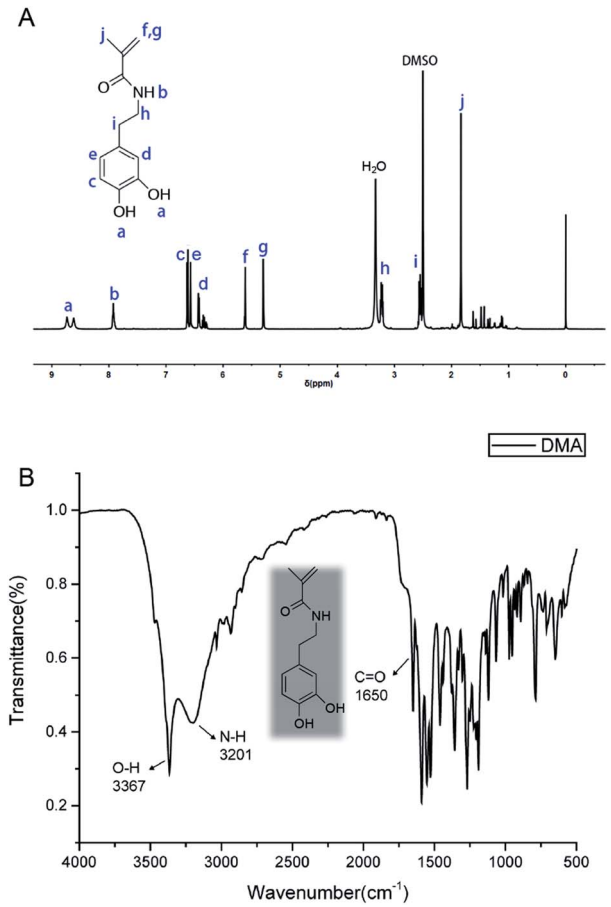

Fig. 4 (A) ^1H NMR spectra of DMA monomer in DMSO. (B) FTIR spectra of DMA monomer.

2 Thermal characterization

Assessment of the thermal properties of the DMA monomer is important to assess its applicability in the oral environment. TGA was carried out to investigate the thermal performance of the DMA monomer. Fig. 5 shows the TGA thermograms of the DMA monomer. An initial degradation temperature of 5% weight loss was observed at 218.34 °C. The maximum tolerant temperature of the oral mucosa is approximately 60 °C. Therefore, the DMA monomer can be applied to the oral environment.

3 Shear bond strength

Previous research has studied a polydopamine coating utilizing dip-coating techniques to immerse the surface into a dopamine-containing aqueous solution with a pH of approximately 8–8.5 for a few hours to allow completion of the auto-oxidative crosslinking reaction.[28] This coating improves adhesion but does not form a direct chemical bond.[25,44] The coating technique differs from the natural bonding principle of mussels and is not capable of replicating the high-strength bonding of the mussels. Only a small number of scientists have attempted to simulate the priming bonding mechanism of natural mussels.[38,39]

In this study, we attempted to apply self-assembled monolayers to provide dynamic interactions (*e.g.*, hydrogen bonds) at the molecular interface level, similar to nature. This study tried to prove whether the simplified molecular analogs could improve the performance of adhesive bonding properties. The DMA primer monomer (small bifunctional group molecules containing catechol and acrylic groups at opposite ends) was prepared to mimic the interaction between the catechol group and the mineral interface of marine mussels. The primer was designed to be attached to the surface of the substrate to

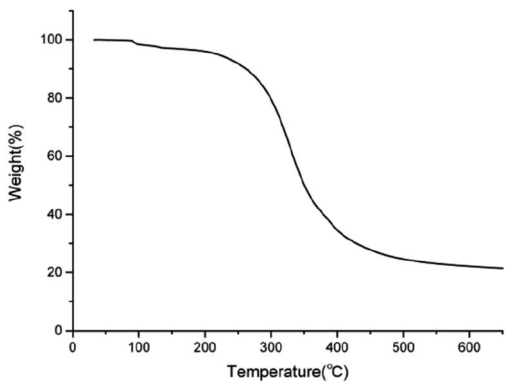

Fig. 5 TGA spectra of DMA monomer powder.

provide chemical crosslinking for two different materials and was prepared using commercially available, inexpensive, naturally sufficient compounds to achieve a more viable and functional system.

Fig. 6 shows the shear strength of three commercial adhesives with different concentrations of DMA primer in different solvents. The application of DMA primer can significantly improve the shear strength when compared with that of the control group and pure solvent group ($p < 0.05$), although there is no difference in shear strength between different concentrations. The difference in DMA primer solvent has no effect on the shear strength of adhesives, which can be seen in Table 3.

We attribute the augmentation of shear strength to the increasing surface physicochemical bonding density of the bidentate hydrogen bonding of catechol groups.[45] The bonding longevity of bidentate hydrogen bonding of catechol group was considered to be 10^6 times longer than a single hydrogen bonding, providing strong and lasting adhesion.[46] Previous studies have shown that catechol groups are easily adsorbed and bound to the surface of hydroxyapatite (HA), which is the main component of the tooth, as shown in Fig. 7(A). In addition to the strong bidentate hydrogen bond, there may be a strong noncovalent bond, such as a π-cation interaction, between benzene rings of catechol groups and Ca^{2+} of HA.[47] Functional monomers containing catechol groups can form a uniform self-assembled monolayer molecular structure.[48] When the dihydroxyl group of catechol combined with dentin through bidentate hydrogen bonding, the methacrylic group on the other end was exposed to the outside, and it could form a chemical bonding with commercial adhesives *via* radical polymerization.[40] Therefore, chemical bonding was formed between the adhesive and dentin apart from mechanical interlocking.

In addition, Ryu. J and colleagues have shown that adequate catechol groups have two functions: a molecule can anchor on a variety of substrates (the catechol group at the interface plays this role) or it can bind with free Ca^{2+} (the catechol group not participating in the interfacial adhesion) and concentrated Ca^{2+}, providing a nucleation site for the formation of hydroxyapatite and the promotion of mineralization,[49] as shown in Fig. 7(B).

Fang. H *et al.* showed that MAP inhibited bacterial collagenase, probably because of the catechol group of DOPA. The catechol group has a strong metal chelation ability, so MAP may competitively chelate Ca^{2+}, which is necessary for bacterial collagenase activity,[50] as shown in Fig. 7(C). As a powerful crosslinking agent, collagen fibers may be cross-linked by covalent bonds between the catechol groups and amino groups of the collagen fibers. The crosslinking hardens the collagen fibers and prevents their triple-helix conformation from unfastening,[51] making crosslinked collagen more resistant to the degradation of collagenase. Therefore, the catechol group can inhibit the activity of collagenase and prevent the degradation of dentin collagen, leading to the enhancement of bonding strength and the postponing of deterioration of adhesion between dentin and composite resin.

Studies have shown that mfp-5 is the first protein that interacts with the substrates and can remove water molecules on the surface before forming a coordination complex with the metal oxide/hydroxide, overcoming repulsive hydration and producing strong surface adhesion,[52] as shown in Fig. 7(D). However, whether the small molecule with the catechol group has the same effect requires further verification.

The failure modes of fracture under the stereomicroscope in this study were adhesive failure, cohesive failure in dentin and mixed failure without cohesive failure in composite resin. Photos of the three fracture modes are shown in Fig. 8(A–C). The distribution of the three fracture modes are shown in Fig. 8 (SB2, SPB, SBU). Most of the results revealed mixed fracture modes (partially adhesive failure and partially cohesive failure), while cohesive failure and adhesive failure showed a lower proportion. Cohesive failure is more likely to occur when the bonding strength exceeds 20 MPa.[53] Previous studies have shown that lower bonding strength presents adhesive failures, while higher bonding strength tends to mixed or cohesive failure.[54] However, in this experiment, the law of the fracture mode and influencing factors are not obvious, probably because of the small sample content.

In conclusion, dentin was effectively modified with the application of DMA primer, which led to enhanced bonding strength and decreased adhesion failure. Although different solvents have no significant effect on the shear strength, ethanol is more volatile than DMSO. Therefore, multiple dipping in primer was required to ensure the wetting of the dentin surface in the treatment time of 60 seconds, which is not

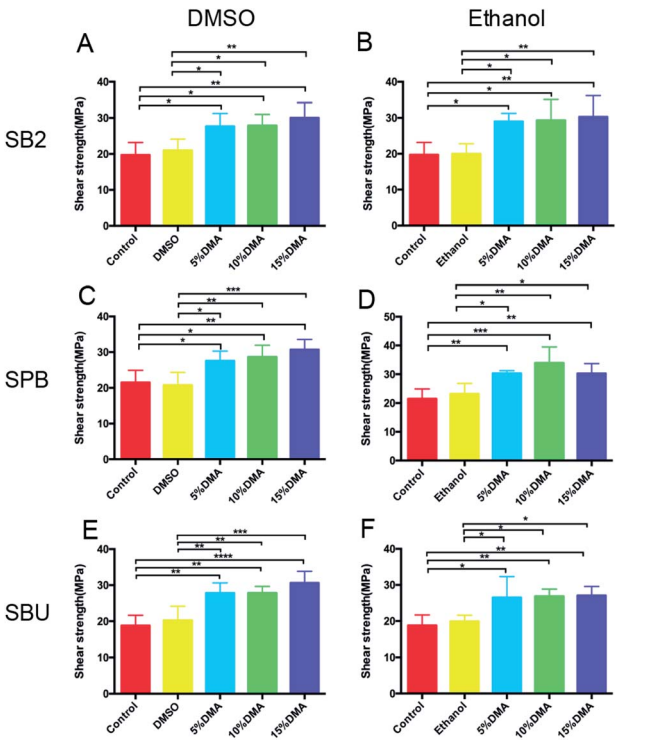

Fig. 6 Shear bond strength (A–F) of the different experimental grouping. The specific grouping of the experiment was shown in Table 1 ($n = 10$).

Table 3 The shear strength ($\bar{X} \pm S$, $n = 10$) of adhesives using different solvents for DMA primer[a]

	SB2			SPB			SBU		
	5% DMA	10% DMA	15% DMA	5% DMA	10% DMA	15% DMA	5% DMA	10% DMA	15% DMA
DMSO	27.69 ± 3.56a	27.84 ± 3.11a	30.04 ± 4.18a	27.59 ± 2.71a	28.65 ± 3.31a	30.72 ± 2.83a	27.79 ± 2.81a	27.79 ± 1.85a	30.60 ± 3.23a
Ethanol	29.02 ± 2.22a	29.31 ± 5.78a	30.28 ± 5.87a	30.33 ± 0.96a	33.95 ± 5.54a	30.28 ± 3.46a	26.52 ± 5.80a	26.86 ± 2.00a	27.07 ± 2.50a

[a] Same lowercase letters in the same column represented no significantly difference ($P > 0.05$) between different solvents.

convenient for clinicians in practice. Therefore, DMSO was chosen as the solvent of primer.

4 Degree of conversion

The DC of the dental adhesive is closely related to the structure of the monomer and the polymerization condition.[55] However, in the present study, these factors were consistent. The only variable that affects DC is whether there is DMA primer application. The results of DC of the three commercial adhesives before and after the use of DMA primer are shown in Fig. 9. For SB2 and SPB, DC was significantly lower ($p < 0.05$) after applying DMA primer, decreasing with the concentration of DMA primer from 5% to 15%. The apparent decrease of DC for SBU was not significant.

The decrease in DC may be because the DMA primer contains a catechol group that can react with a free radical. Thus, the catechol group can act as a free radical scavenger, affecting the polymerization of commercial adhesive monomers.[40,56] Inadequate polymerization of adhesives accelerates water degradation, leading to bonding failure.[57,58] Therefore, a lower concentration of 5% DMA primer was chosen for the follow-up experiment.

5 Contact angle measurements

The wettability of the surface after application of the DMA primer was characterized by testing the static water contact angle, as shown in Fig. 9. The contact angle of the dentin revealed a significant decrease ($p < 0.05$) from 87.37 ± 5.28° to 62.23 ± 4.85° after priming the dentin with DMA primer, indicating the improvement of wettability of the demineralized dentin, which promotes adhesives to better wet and penetrate into the hybrid layer of demineralized dentin, benefiting the bonding adhesion.[59] It is worth mentioning that the wettability tested in this study is actually attributable to the performance of the DMA primer applied to the dentin.

The catechol group at one end of the DMA primer interacts with dentin, and the vinyl carbon–carbon double bond (–CH=CH_2) at the other end is exposed to the outside, which is a hydrophobic group. This should increase the contact angle, but the solvent component of the DMA primer plays a major

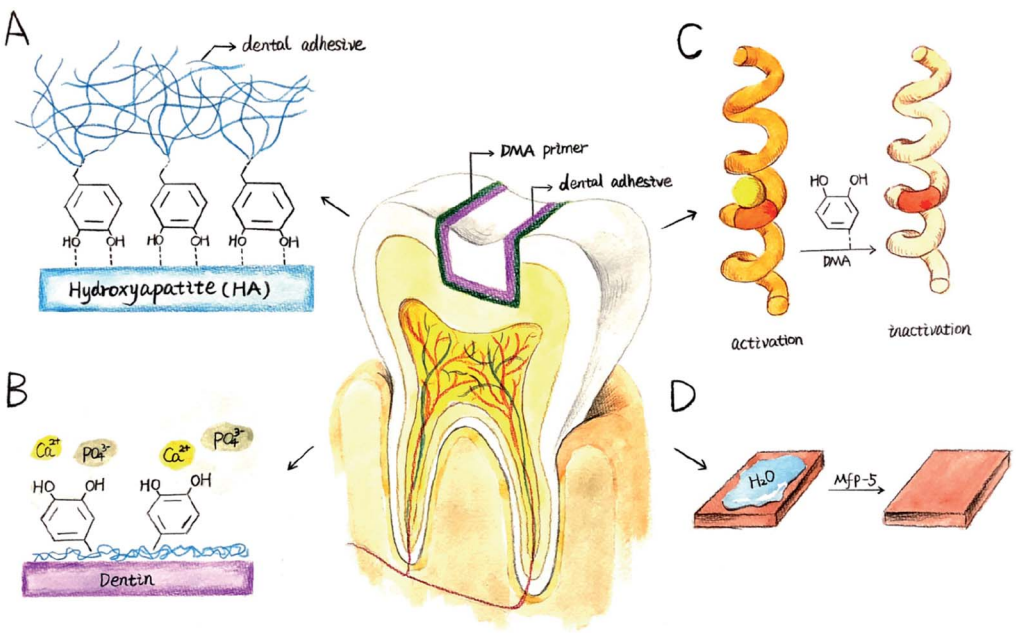

Fig. 7 The possible mechanism of augmentation of shear strength after using DMA primer. (A) Catechol groups are easily adsorbed to the surface of hydroxyapatite (HA) by bidentate hydrogen bonding; (B) the catechol group can also bind with free Ca^{2+} and concentrated Ca^{2+}, promoting mineralization; (C) the catechol group has a strong metal chelation ability, competitively chelate Ca^{2+}, inhibited bacterial collagenase; (D) mfp-5 can remove water molecules on the surface before forming a coordination complex with substrate.

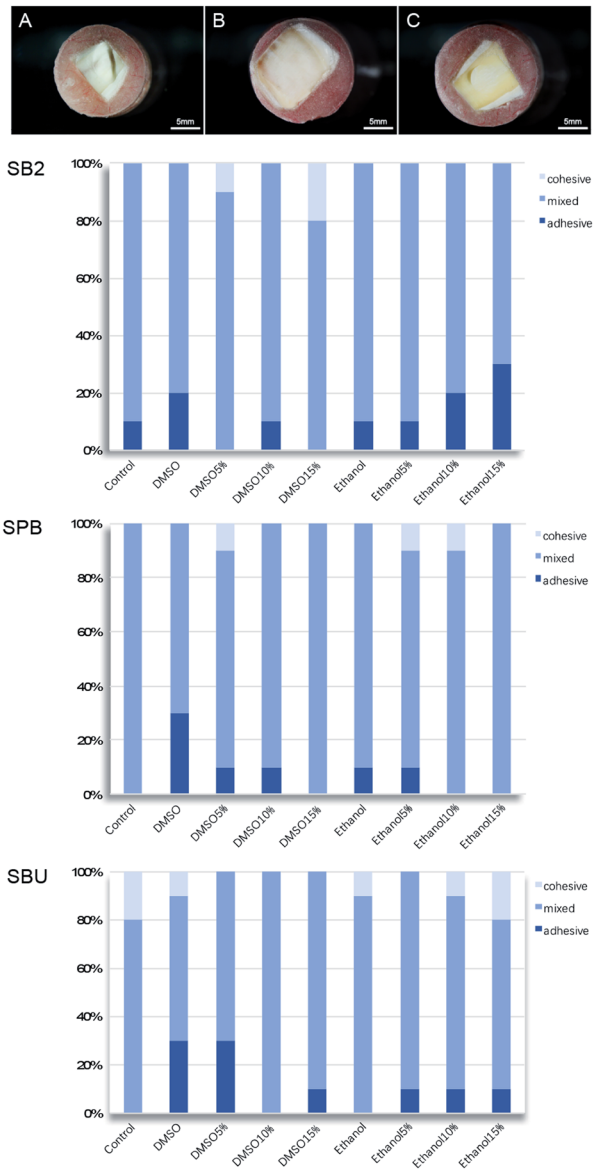

Fig. 8 (A) Cohesive failure in dentin; (B) adhesive failure; (C) mixed failure; distribution of three fracture modes (SB2, SPB, SBU).

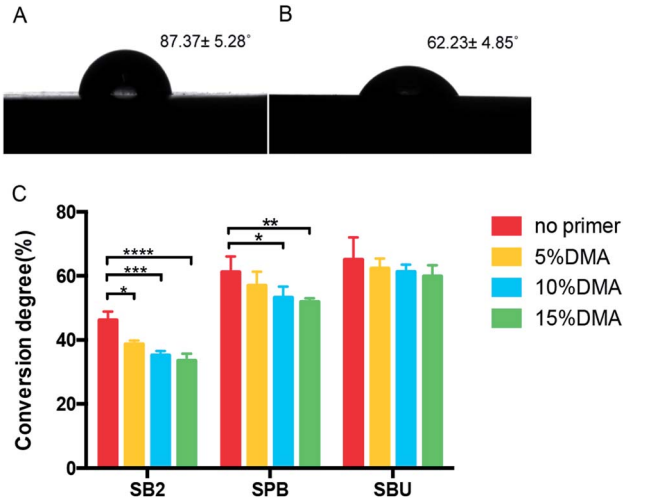

Fig. 9 Representative images of contact angle on the bovine dentin surface (A) contact angle without primer = 87.37 ± 5.28°; (B) contact angle with primer = 62.23 ± 4.85°; (C) influence of the DMA primer on degree of conversion of the commercial adhesive.

role in improving the wettability, compensating for the hydrophobility of the vinyl carbon–carbon double bond. The interaction force of DMSO–water is 1.3 times more powerful than that of the water–water bond. The oxygen atom at one end of the DMSO molecule is capable of forming a hydrogen bond with two water molecules in a hydrophilic manner. The methyl group at the other end without charge could lead to the formation of a lattice by water molecules around it in a hydrophobic manner.[60] Therefore, the DMSO molecule can cause a breakage of the water self-association, reducing the surface tension and cohesion of water, thus improving the liquid wettability. DMSO is a good wetting agent, especially for irregular surfaces with voids, due to its high dielectric constant, low surface tension and balance of polarity and surface tension properties.[61]

6 Microleakage in composite restoration

Microleakage between the tooth and composite resin restoration is the factor leading to restoration failure.[62] Bacteria can leak into the gap and dentinal tubule *via* microleakage, leading to the occurrence of secondary caries and stimulation of the pulp tissue. The oral environment (including changes in occlusal force and temperature) and different physical properties between teeth and restorative materials (including polymerization shrinkage, coefficient of thermal expansion and modulus of elasticity,[63] dissolution of bonding or repairing materials,[64] and dissolution of lining or mixed layers[65]) can cause microleakage.

In this experiment, microleakage was significantly decreased after the application of DMA primer, which could be observed in Fig. 10. The microleakage of group A and group C reached the axial surface with depths of 2.21 ± 0.39 mm and 2.71 ± 0.41 mm, respectively. The leakage of group E exceeded half of the depth of the hole, reaching 1.50 ± 0.31 mm, while Group B did not reach half of the depth of the hole, at only 0.67 ± 0.21 mm. No significant microleakage was observed in the D and F groups.

The initial marginal gap between the tooth and composite is derived from the polymerization shrinkage of the restorative materials.[66] Therefore, if the adhesion to the tooth surface is weaker than the stress generated by the polymerization shrinkage of the adhesive and composite, a tiny gap between the tooth and adhesive will form, leading to restoration failure.[66] The improvement of the bonding strength after application of DMA primer also improves the microleakage performance of the adhesive. In this experiment, evaluation of microleakage and evaluation of shear strength are combined to provide a more comprehensive evaluation of bonding performance. Previous studies have shown a negative correlation between microleakage and shear strength,[67] consistent with the results of this study.

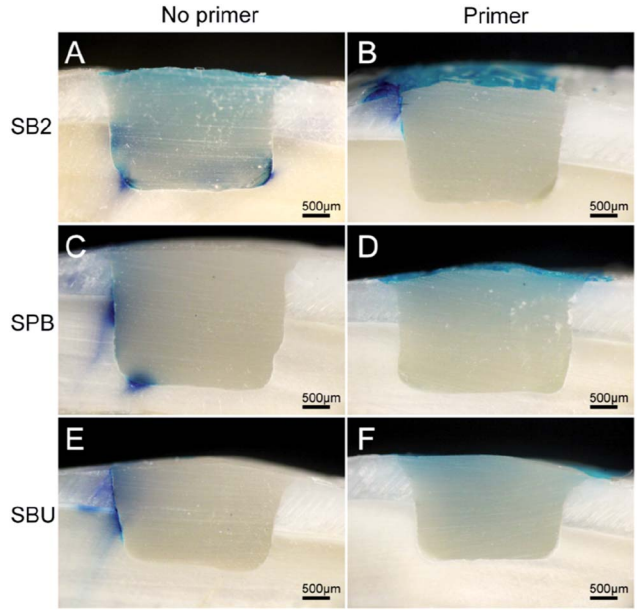

Fig. 10 Microleakage between dentin and composite resins after 5000 thermocycling. A (SB2, no primer); B (SB2, primer); C (SPB, no primer); D (SPB, primer); E (SBU, no primer); F (SBU, primer). Bar = 500 μm.

7 Biocompatibility of DMA primer

The toxicity of the DMA primer toward L929 was evaluated by cell activity and morphological changes. As shown in Fig. 11(A), there was no significant difference ($p > 0.05$) between the experimental group and the control group in terms of cell proliferation activity after different culture times. A relative survival rate greater than 70% can be considered to be nontoxic.[42] The relative cell viability in this experiment was all greater than 85%. However, most are lower than the control group, probably because a small portion of the catechol groups will oxidize to form a highly reactive quinone group that can react with the protein of the cell membrane. At the same time, reactive oxygen is generated, for example, superoxide anion (O^{2-}) and hydrogen peroxide (H_2O_2), which are toxic to cells.[68]

As shown in Fig. 11(B), the effect of DMA primer on cell proliferation activity was quantified by a live/dead staining experiment, and cells were counted using ImageJ software. The proportion of viable cells in the experimental group was similar to that in the control group. The results obtained from MTT are consistent with the live/dead staining experiment. The morphology of L929 cells was observed after culturing for 24 h with different concentrations of DMA primer, as shown in Fig. 11(B). After incubation for 24 h, L929 cells were lengthened and became spindle-shaped, which was similar to the typical fibroblasts in the control group, indicating that cells presented well-stretched actin bundles. The cell culture was evenly distributed, and the intercellular spaces did not change significantly. In general, the DMA primer was nontoxic to L929 cells, which established a good foundation for the future clinical application of catecholic primers.

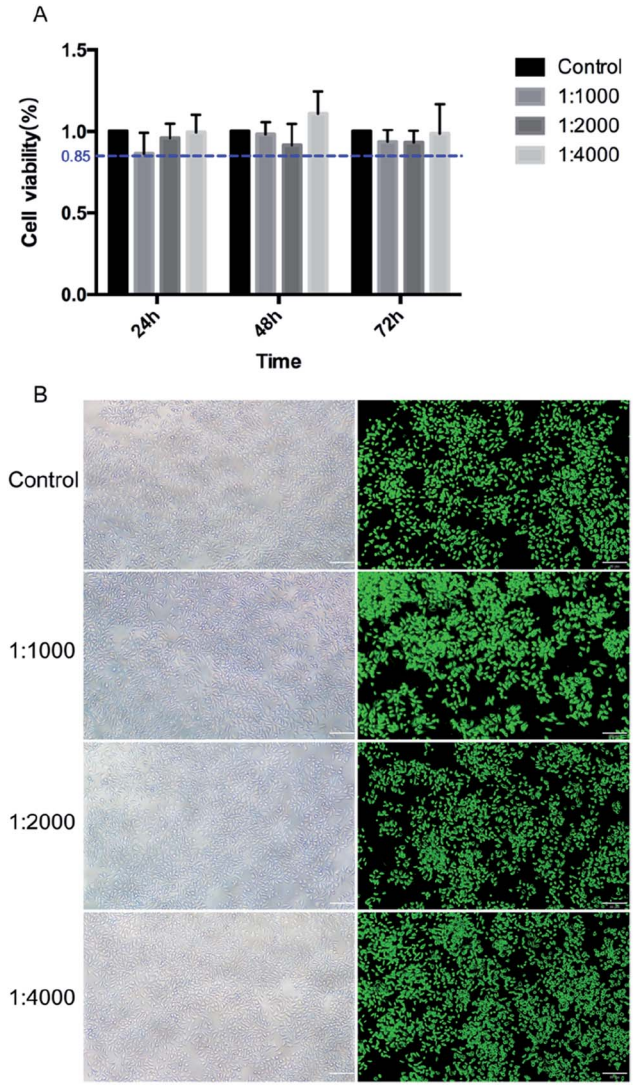

Fig. 11 (A) Cytotoxicity of the 5% DMA primer in different dilutions with culture medium at 24 h, 48 h, 72 h was determined by MTT assay. (B) Optical microscopy images (left) and live/dead fluorescence cell staining (right) after L929 cells were cultured for 24 h in culture medium (control), 5% DMA primer in different dilutions (1 : 1000, 1 : 2000, and 1 : 4000 (v/v) dilutions). Living cells were stained by calcium-AM (green), and dead cells were stained by PI (red). Scale bars = 100 μm.

Conclusions

In summary, we prepared a biomimic catecholic DMA primer with a bifunctional group, imitating the adhesion mechanism of marine mussels. The shear bond strength was significantly improved, and microleakage was diminished after introducing the catechol group into the dentin primer. Studies have shown that 5% DMA primer using DMSO solvent has a better comprehensive performance. This study lays the foundation for the application of DMA primers in clinical practice, intending for strong and long-lasting adhesion.

Conflicts of interest

There are no conflicts to declare.

Acknowledgements

This research was financially supported by the National Natural Science Foundation of China (NSFC, Grant No. 81671033).

Notes and references

1 C. D. Lynch, N. J. Opdam, R. Hickel, P. A. Brunton, S. Gurgan, A. Kakaboura, A. C. Shearer, G. Vanherle and N. H. F. Wilson, *J. Dent.*, 2014, **42**, 377–383.
2 J. L. Ferracane, *Dent. Mater.*, 2011, **27**, 29–38.
3 J. L. Drummond, *J. Dent. Res.*, 2008, **87**, 710–719.
4 D. C. Watts, A. S. Marouf and A. M. Al-Hindi, *Dent. Mater.*, 2003, **19**, 1–11.
5 S. C. Bayne, J. Y. Thompson, E. J. Swift, P. Stamatiades and M. Wilkerson, *J. Am. Dent. Assoc.*, 1998, **129**, 567–577.
6 D. H. Pashley, F. R. Tay, L. Breschi, L. Tjäderhane, R. M. Carvalho, M. Carrilho and A. Tezvergil-Mutluay, *Dent. Mater.*, 2011, **27**, 1–16.
7 B. Van Meerbeek, K. Yoshihara, Y. Yoshida, A. Mine, J. De Munck and K. L. Van Landuyt, *Dent. Mater.*, 2011, **27**, 17–28.
8 L. Breschi, A. Mazzoni, A. Ruggeri, M. Cadenaro, R. Di Lenarda and E. De Stefano Dorigo, *Dent. Mater.*, 2008, **24**, 90–101.
9 P. Spencer, Q. Ye, J. Park, E. M. Topp, A. Misra, O. Marangos, Y. Wang, B. S. Bohaty, V. Singh, F. Sene, J. Eslick, K. Camarda and J. L. Katz, *Ann. Biomed. Eng.*, 2010, **38**, 1989–2003.
10 S. Imazato, F. R. Tay, A. V. Kaneshiro, Y. Takahashi and S. Ebisu, *Dent. Mater.*, 2007, **23**, 170–176.
11 J. L. Ferracane, *Dent. Mater.*, 2013, **29**, 51–58.
12 B. S. Bohaty, Q. Ye, A. Misra, F. Sene and P. Spencer, *Clin., Cosmet. Invest. Dent.*, 2013, **5**, 33–42.
13 P. Spencer, Q. Ye, A. Misra, S. E. P. Goncalves and J. S. Laurence, *J. Dent. Res.*, 2014, **93**, 1243–1249.
14 Y. Delaviz, Y. Finer and J. P. Santerre, *Dent. Mater.*, 2014, **30**, 16–32.
15 R. Osorio, E. Osorio, A. Medina-Castillo and M. Toledano, *J. Dent. Res.*, 2014, **93**, 1258–1263.
16 Y. Liu, L. Tjäderhane, L. Breschi, A. Mazzoni, N. Li, J. Mao, D. H. Pashley and F. R. Tay, *J. Dent. Res.*, 2011, **90**, 953–968.
17 Q. X. Liu, P. M. Herman, W. M. Mooij, J. Huisman, M. Scheffer, H. Olff and J. Van De Koppel, *Nat. Commun.*, 2014, **5**, 5234.
18 T. W. Gilbert and E. D. Sone, *Biofouling*, 2010, **26**, 829–836.
19 E. Hennebert, B. Maldonado, P. Ladurner, P. Flammang and R. Santos, *Interface Focus*, 2015, **5**, 20140064.
20 E. Hennebert, R. Wattiez, M. Demeuldre, P. Ladurner, D. S. Hwang, J. H. Waite and P. Flammang, *Proc. Natl. Acad. Sci.*, 2014, **111**, 6317–6322.
21 B. P. Lee, P. B. Messersmith, J. N. Israelachvili and J. H. Waite, *Annu. Rev. Mater. Res.*, 2011, **41**, 99–132.
22 H. G. Silverman and F. F. Roberto, *Mar. Biotechnol.*, 2007, **9**, 661–681.
23 J. H. Waite, N. H. Andersen, S. Jewhurst and C. Sun, *J. Adhes.*, 2005, **81**, 297–317.
24 D. S. Hwang, H. Zeng, A. Masic, M. J. Harrington, J. N. Israelachvili and J. H. Waite, *J. Biol. Chem.*, 2010, **285**, 25850–25858.
25 B. K. Ahn, S. Das, R. Linstadt, Y. Kaufman, N. R. Martinez-Rodriguez, R. Mirshafian, E. Kesselman, Y. Talmon, B. H. Lipshutz, J. N. Israelachvili and J. Herbert Waite, *Nat. Commun.*, 2015, **6**, 8663.
26 L. Ninan, J. Monahan, R. L. Stroshine, J. J. Wilker and R. Shi, *Biomaterials*, 2003, **24**, 4091–4099.
27 J. H. Waite and S. O. Andersen, *Biochim. Biophys. Acta*, 1978, **541**, 107–114.
28 H. Lee, S. M. Dellatore, W. M. Miller and P. B. Messersmith, *Science*, 2007, **318**, 426–430.
29 C. Xu, K. Xu, H. Gu, R. Zheng, H. Liu, X. Zhang, Z. Guo and B. Xu, *J. Am. Chem. Soc.*, 2004, **126**, 9938–9939.
30 B. K. Ahn, D. W. Lee, J. N. Israelachvili and J. H. Waite, *Nat. Mater.*, 2014, **13**, 867–872.
31 C. Gao, G. Li, H. Xue, W. Yang, F. Zhang and S. Jiang, *Biomaterials*, 2010, **31**, 1486–1492.
32 S. B. Lee, C. González-Cabezas, K. M. Kim, K. N. Kim and K. Kuroda, *Biomacromolecules*, 2015, **16**, 2265–2275.
33 E. Shin, S. W. Ju, L. An, E. Ahn, J. S. Ahn, B. S. Kim and B. K. Ahn, *ACS Appl. Mater. Interfaces*, 2018, **10**, 1520–1527.
34 E. Filippidi, D. G. DeMartini, P. Malo de Molina, E. W. Danner, J. Kim, M. E. Helgeson, J. H. Waite and M. T. Valentine, *J. R. Soc., Interface*, 2015, **12**, 20150827.
35 C. R. Matos-Pérez, J. D. White and J. J. Wilker, *J. Am. Chem. Soc.*, 2012, **134**, 9498–9505.
36 M. Mehdizadeh, H. Weng, D. Gyawali, L. Tang and J. Yang, *Biomaterials*, 2012, **33**, 7972–7983.
37 Y. Li, H. Meng, Y. Liu, A. Narkar and B. P. Lee, *ACS Appl. Mater. Interfaces*, 2016, **8**, 11980–11989.
38 L. Hamming, X. Fan, P. Messersmith and L. C. Brinson, *Compos. Sci. Technol.*, 2008, **68**, 2042–2048.
39 M. Yi, H. Sun, H. Zhang, X. Deng, Q. Cai and X. Yang, *Mater. Sci. Eng., C*, 2016, **58**, 742–749.
40 S. Seo, D. W. Lee, J. S. Ahn, K. Cunha, E. Filippidi, S. W. Ju, E. Shin, B. S. Kim, Z. A. Levine, R. D. Lins, J. N. Israelachvili, J. H. Waite, M. T. Valentine, J. E. Shea and B. K. Ahn, *Adv. Mater.*, 2017, **29**, 1703026.
41 X. Wang, S. Jing, Y. Liu, S. Liu and Y. Tan, *Polymer*, 2017, **116**, 314–323.
42 D. Cao, Y. Zhang, Y. Li, X. Shi, H. Gong, D. Feng, X. Guo, Z. Shi, S. Zhu and Z. Cui, *Mater. Sci. Eng., C*, 2017, **78**, 333–340.
43 R. S. Chen, C. C. Liu, W. Y. Tseng, J. H. Jeng and C. P. Lin, *J. Dent.*, 2003, **31**, 223–229.
44 Q. Lin, D. Gourdon, C. Sun, N. Holten-Andersen, T. H. Anderson, J. H. Waite and J. N. Israelachvili, *Proc. Natl. Acad. Sci.*, 2007, **104**, 3782–3786.
45 J. Yu, Y. Kan, M. Rapp, E. Danner, W. Wei, S. Das, D. R. Miller, Y. Chen, J. H. Waite and J. N. Israelachvili, *Proc. Natl. Acad. Sci.*, 2013, **110**, 15680–15685.
46 J. Yu, W. Wei, E. Danner, R. K. Ashley, J. N. Israelachvili and J. H. Waite, *Nat. Chem. Biol.*, 2011, **7**, 588–590.

47 W. Wei, L. Petrone, Y. Tan, H. Cai, J. N. Israelachvili, A. Miserez and J. H. Waite, *Adv. Funct. Mater.*, 2016, **26**, 3496–3507.
48 S. Das, B. H. Lee, R. T. Linstadt, K. Cunha, Y. Li, Y. Kaufman, Z. A. Levine, B. H. Lipshutz, R. D. Lins, J. E. Shea, A. J. Heeger and B. K. Ahn, *Nano Lett.*, 2016, **16**, 6709–6715.
49 J. Ryu, S. H. Ku, H. Lee and C. B. Park, *Adv. Funct. Mater.*, 2010, **20**, 2132–2139.
50 H. Fang, Q. L. Li, M. Han, M. L. Mei and C. H. Chu, *Dent. Mater.*, 2017, **33**, 1075–1083.
51 C. Sabatini and D. H. Pashley, *Am. J. Dent.*, 2014, **27**, 203–214.
52 L. Petrone, A. Kumar, C. N. Sutanto, N. J. Patil, S. Kannan, A. Palaniappan, S. Amini, B. Zappone, C. Verma and A. Miserez, *Nat. Commun.*, 2015, **6**, 8737.
53 R. F. Schreiner, R. P. Chappell, A. G. Glaros and J. D. Eick, *Dent. Mater.*, 1998, **14**, 194–201.
54 S. S. Scherrer, P. F. Cesar and M. V. Swain, *Dent. Mater.*, 2010, **26**, e78–e93.
55 L. Hong, Y. Wang, L. Wang, H. Zhang, H. Na and Z. Zhang, *J. Dent.*, 2017, **59**, 11–17.
56 Q. Zhang, G. Nurumbetov, A. Simula, C. Zhu, M. Li, P. Wilson, K. Kempe, B. Yang, L. Tao and D. M. Haddleton, *Polym. Chem.*, 2016, **7**, 7002–7010.
57 V. Hass, M. Dobrovolski, C. Zander-Grande, G. C. Martins, L. A. Gordillo, M. L. R. Accorinte, O. M. Gomes, A. D. Loguercio and A. Reis, *Dent. Mater.*, 2013, **29**, 921–928.
58 M. Cadenaro, F. Antoniolli, B. Codan, K. Agee, F. R. Tay, E. S. Dorigo, D. H. Pashley and L. Breschi, *Dent. Mater.*, 2010, **26**, 288–294.
59 J. Guo, W. Lei, H. Yang, Y. Zhang, S. Zhao and C. Huang, *J. Adhes. Dent.*, 2017, **19**, 229–237.
60 P. Mehtälä, D. H. Pashley and L. Tjäderhane, *Dent. Mater.*, 2017, **33**, 915–922.
61 R. Redon, A. Vázquez-Olmos, M. Mata-Zamora, A. Ordóñez-Medrano, F. Rivera-Torres and J. M. Saniger, *J. Colloid Interface Sci.*, 2005, **287**, 664–670.
62 K. Jang, D. Chung, D. Shin and F. García-Godoy, *Operat. Dent.*, 2001, **26**, 603–608.
63 J. Manhart, H. Y. Chen, A. Mehl, K. Weber and R. Hickel, *J. Dent.*, 2001, **29**, 123–130.
64 P. Mason, M. Ferrari, M. Cagidiaco and C. L. Davidson, *J. Dent.*, 1996, **24**, 217–222.
65 D. Fortin, E. J. Swift Jr, G. E. Denehy and J. W. Reinhardt, *Dent. Mater.*, 1994, **10**, 253–258.
66 C. Davidson, A. J. De Gee and A. Feilzer, *J. Dent. Res.*, 1984, **63**, 1396–1399.
67 C. Prati, M. Simpson, J. Mitchem, L. Tao and D. H. Pashley, *Dent. Mater.*, 1992, **8**, 37–41.
68 Z. Zeng, H. Wang, Y. Morsi and X. Mo, *Colloids Surf., B*, 2018, **161**, 94–102.

